New Satellite Method for Retrieving Precipitable Water Vapor over Land and Ocean

Merritt N. Deeter

Research Applications Laboratory

National Center for Atmospheric Research

Boulder, CO, USA

Merritt N. Deeter, Research Applications Laboratory, National Center for Atmospheric Research, Boulder, CO 80307 (mnd@ucar.edu)

A fundamentally new method is presented for retrieving precipitable water vapor (PWV) using observations from the Advanced Microwave Scanning Radiometer for EOS (AMSR-E) satellite instrument. Unlike all existing passive satellite methods, the new technique is applicable both day and night, over ocean and land surfaces, and with little sensitivity to clouds. The method relies on a simple but accurate parameterization which relates AMSR-E polarization-difference signals at 18.7 and 23.8 GHz to PWV, liquid water path and the surface emissivity polarization difference. Over land, validation is based on comparisons with the SuomiNet network of ground-based GPS receivers. With quality control measures applied, RMS retrieval errors over land are limited to approximately six mm with a linear correlation coefficient of 0.89. Differences with the operational AMSR-E oceanic PWV product are typically less than two mm. Products based on the new method should prove valuable in weather and climate research.

1. Introduction

Satellite-based observations of water vapor are used widely in studies of weather and climate [e.g., Stephens, 1990; Trenberth et al., 2005]. Passive methods for retrieving precipitable water vapor PWV (i.e., the vertical integral of the water vapor mixing ratio) exploit water vapor absorption bands in three distinct spectral domains. Methods based on solar reflectance (SR) channels rely on absorption between about 0.9 and 1.0 μm [Gao and Kaufman, 2003; Albert et al., 2005]. Methods based on thermal-infrared (TIR) channels rely on absorption and emission between about 6.5 and 8.7 μm [e.g., Seemann et al., 2003]. Finally, microwave (MW) techniques for retrieving PWV typically exploit water vapor absorption lines at either 22.2 or 183.3 GHz (corresponding to wavelengths of 1.35 cm and 1.64 mm) [Sohn and Smith, 2003; Engelen and Stephens, 1999]. Microwave-based products are often favored in climate studies because they are not affected by the "clear-sky bias" inherent to the SR and TIR methods [Stephens et al., 1994; Simpson et al., 2001].

Despite the variety of methods for retrieving PWV from space-based platforms, there are still common situations for which existing methods are not applicable. In particular, standard methods can not be applied over land surfaces obscured by clouds (either day or night). This paper describes a new microwave-based method which fills this void. The new method exploits unique capabilities of the Advanced Microwave Scanning Radiometer EOS (AMSR-E) on the NASA Aqua platform [Kawanishi et al., 2003]. This conical-scanning instrument separately measures H- and V-polarized brightness temperatures at

both 18.7 and 23.8 GHz. The dual-polarization capability is a key to the new retrieval algorithm.

AMSR-E polarization-difference signals at 18.7 and 23.8 GHz are the only measurements used in the new PWV retrieval method. Previous radiative transfer modeling [Deeter and Vivekanandan, 2006] demonstrated that AMSR-E polarization-difference signals ($\Delta T_B = T_B^V$ - T_B^H) at 36.5 and 89.0 GHz could be accurately parameterized in terms of two atmospheric parameters (PWV and liquid water path LWP) and two surface parameters (surface temperature T_S and surface emissivity polarization difference $\Delta\epsilon = \epsilon^V$ - ϵ^H). Below, we demonstrate that polarization-difference signals for the AMSR-E 18.7 and 23.8 GHz channels can be similarly parameterized. Consequently, both signals are (1) proportional to $\Delta\epsilon$ and (2) exponentially dependent on PWV. The surface parameter $\Delta\epsilon$ exhibits considerable spatial variability due to vegetation, soil moisture and other factors, but is only weakly frequency-dependent; we assume this variable is frequency-independent between 18 and 24 GHz. However, because of their spectral positions relative to the water vapor absorption line at 22.2 GHz, the 23.8 GHz polarization difference signal is significantly more sensitive to water vapor concentrations than is the signal at 18.7 GHz. As a result, the ratio of the AMSR-E polarization-difference signals at 18.7 and 23.8 GHz is sensitive to PWV but not to surface parameters.

2. Algorithm Theoretical Basis

2.1. Polarization-Difference Parameterization

The Polarization-Difference Parameterization (PDP) was previously developed to enable a LWP retrieval algorithm based on AMSR-E observations at 36.5 and 89.0 GHz

[Deeter and Vivekanandan, 2006]. Here we show that the same parameterization accurately models AMSR-E ΔT_B signals at 18.7 and 23.8 GHz. The PDP takes the form

$$\boldsymbol{\Delta T_B \approx \Delta\epsilon \exp(\beta_0 + \beta_1 T_S + \beta_2 LWP + \beta_3 PWV)} \tag{1}$$

where the β_i values are frequency-dependent regression coefficients determined by applying multiple linear regression to radiative transfer simulations. The "training set" used in the simulations was based on randomly-drawn profiles from NCEP Reanalysis for a region covering most of North America and surrounding oceanic areas (bounded by 30N, 60N, 130W and 60W) for all of 2001. Values of the PDP regression coefficients β_i for the AMSR-E 18.7 and 23.8 GHz channels are listed in Table 1. The fit of the regression is shown graphically in Fig. 1. Plotted data in each panel correspond to the individual training-set profiles (and model-calculated brightness temperatures) which are the basis of the regression. Solid lines indicate the best-fit result from multiple linear regression. Figure 1 indicates that the PDP accurately models the AMSR-E polarization-difference signals at 18.7 and 23.8 GHz over widely varying continental and marine atmospheric states.

2.2. Retrieval Equation

Application of the PDP to AMSR-E observations at both 18.7 and 23.8 GHz yields two equations with five unknowns: T_S, LWP, PWV, $\Delta\epsilon^{19}$ and $\Delta\epsilon^{24}$. (The superscripts "19" and "24" refer to the 18.7 and 23.8 GHz channels respectively.) Solving for PWV yields the result

$$\boldsymbol{PWV = \frac{\ln(\frac{\Delta T_B^{24}}{\Delta T_B^{19}}) - \ln(\frac{\Delta\epsilon^{24}}{\Delta\epsilon^{19}}) - (\beta_0^{24} - \beta_0^{19}) - (\beta_1^{24} - \beta_1^{19}) T_S - (\beta_2^{24} - \beta_2^{19}) LWP}{\beta_3^{24} - \beta_3^{19}}} \tag{2}$$

Additional assumptions are then used to further simplify the retrieval equation. First, the sensitivity of PWV to T_S is weak. The partial derivative of PWV with respect to T_S calculated using Eq. 1 and coefficients in Table 1 indicates a sensitivity of 0.0069 mm/K. Thus, an error in T_S of 10 K would produce a PWV retrieval errors of only 0.07 mm. In the following, we assume that reasonably accurate T_S values are available either through observations or forecasts. For results presented in Section 3, we also assume that LWP is exactly 0. The validity of this assumption is discussed in Section 2.3. Finally, we assume that $\Delta\epsilon^{19} = \Delta\epsilon^{24}$. This assumption is supported by several studies based on SSM/I observations over various land surface types which demonstrated that $\Delta\epsilon$ is only weakly frequency-dependent [Prigent et al., 1997; Lin and Minnis, 2000; Ruston and Vonder Haar, 2004].

Under these assumptions, Eq. 2 simplifies to

$$\boldsymbol{PWV} = \frac{\ln(\frac{\boldsymbol{\Delta T_B^{24}}}{\boldsymbol{\Delta T_B^{19}}}) - (\boldsymbol{\beta_0^{24}} - \boldsymbol{\beta_0^{19}}) - (\boldsymbol{\beta_1^{24}} - \boldsymbol{\beta_1^{19}})\boldsymbol{T_S}}{\boldsymbol{\beta_3^{24}} - \boldsymbol{\beta_3^{19}}} \tag{3}$$

The parameter $\Delta\epsilon$ modulates the polarization-difference signals at both 18.7 and 23.8 GHz and therefore affects signal-to-noise ratio. This retrieval byproduct, which is calculated using Eq. 1 (after determining PWV), provides a useful index of retrieval quality.

2.3. Retrieval Errors

A variety of effects might contribute to PWV retrieval errors in the new method. With respect to instrumental effects, measured brightness temperatures (and resulting polarization-difference signals) are subject to processes which produce random noise. The degrading effect of these errors on retrieval quality increases as ΔT_B decreases. Thus, PWV retrieval uncertainties will generally increase as $\Delta\epsilon$ decreases [Deeter and Vivekanan-

dan, 2006]. Retrieval errors due to instrumental noise are controlled in the new method by signal averaging. For the retrieval results presented in Section 3, a rectangular latitude/longitude grid was employed with grid cells measuring 0.25 by 0.25 degrees. Because AMSR-E observations at both 18.7 and 23.8 GHz are sampled every 10 km (both along-track and along the conical scan), approximately 25 independent measurements are averaged in each grid cell. Thus, assuming a square-root reduction in the effective instrumental noise with the number of samples, the effective instrumental noise is reduced from 0.6 K [Kawanishi et al., 2003] to approximately 0.1 K.

Other potential sources of retrieval error include forward model error, parameterization error, errors due to finite LWP, radiative scattering from precipitation, and errors associated with the frequency dependence of $\Delta\epsilon$. From Eq. 2, the calculated sensitivity of the PWV to errors in assumed LWP is 14.5; an error in assumed LWP of 0.1 mm translates to a PWV retrieval error of 1.5 mm. However, in most liquid clouds, values of LWP are significantly less than 0.1 mm. For example, for all LWP retrievals based on a ground-based microwave radiometer at the ARM SGP site over an entire year, the median LWP value was only 0.001 mm. Nevertheless, about 12% of the LWP retrievals in the same dataset exceeded 0.2 mm, which would indicate a retrieval error of 3 mm. Effects of precipitation at 18.7 and 23.8 GHz are weaker than at higher frequencies but might still produce retrieval error. However, retrieval degradation due to precipitation could probably be minimized by using the higher frequency AMSR-E channels to screen affected observations [Wilheit et al., 2003]. However, such a method was not implemented in this study.

Measurements of the frequency dependence of $\Delta\epsilon$ in the spectral interval from 18 to 24 GHz have apparently not been reported for any surface type. However, values of $\Delta\epsilon$ for the SSM/I 19 and 37 GHz channels are available in the literature [Prigent et al., 1997; Lin and Minnis, 2000; Ruston and Vonder Haar, 2004]. Results of those studies indicate that $\Delta\epsilon$ varies by about 10-20% between 19 and 37 GHz. It is reasonable to assume that $\Delta\epsilon$ varies even less between 18 and 24 GHz.

3. Results

Because available PWV datasets lack global coverage, separate datasets were used to validate the PDP-based PWV product over land and ocean. Results presented here are limited to comparisons against (1) PWV measurements over a full year from SuomiNet, a ground-based network of Global Positioning System (GPS) receivers in North America [Ware et al., 2000], and (2) operational AMSR-E over-ocean retrievals [Wentz and Meissner, 2000] for one day. In neither case were any data excluded because of the possible effects of clouds.

3.1. GPS-based Comparisons

For validating PDP-based PWV retrievals over land, observations made either by radiosondes, ground-based microwave radiometers, or ground-based GPS receivers could be exploited. Radiosonde launch points are widely dispersed, but launches typically only occur twice per day and are not synchronized with satellite overpasses. Radiosondes also often perform poorly in very cold environments, such as the upper troposphere. Ground-based microwave radiometers provide a precise means of retrieving PWV continuously, but are deployed only in a few regions such as the ARM SGP site.

A network of continuously-operating GPS receivers known as SuomiNet is comprised of stations located in a wide variety of geographical regions throughout North America [Ware et al., 2000]. GPS-based measurements of PWV exhibit excellent agreement with ground-based microwave radiometer-based products and are characterized by absolute errors less than two mm [Braun et al., 2003]. Moreover, unlike radiometer-based products, GPS-based measurements of PWV are unaffected by precipitation. Therefore, we chose to compare PDP-based PWV retrievals over North America with matched PWV results from SuomiNet stations for all of 2004. Observations from 53 SuomiNet stations were acquired for this study.

For each AMSR-E overpass of a SuomiNet ground station, all AMSR-E observations within a 0.25 by 0.25 latitude/longitude grid cell centered on the station location were extracted and averaged to form mean polarization-difference signals at 18.7 and 23.8 GHz. PWV was calculated along with the byproduct $\Delta\epsilon$ and matched with the Suominet PWV value interpolated to the time of the AMSR-E overpass. PWV retrievals from a total of 25,639 AMSR-E overpasses of Suominet stations during 2004 were processed and matched with corresponding GPS-based PWV values.

Results of the AMSR-E/GPS comparisons are presented as a scatterplot in Fig. 2. Different plotting symbols are used to identify retrievals for which $\Delta\epsilon > 0.03$ (diamonds) and $\Delta\epsilon \leq 0.03$ (plus signs). Larger black diamonds with attached vertical error bars indicate statistics (mean and standard deviation) of matchups where $\Delta\epsilon > 0.03$ in PWV bins spaced every five mm. Also indicated are the least-squares best fit based on matchups where $\Delta\epsilon > 0.03$ (the dashed line) and the line of perfect correlation (the dash-dot line).

Validation statistics, including the number of paired PWV values N, the least-squares best-fit slope m and offset b, the linear correlation coefficient r, and the overall bias and standard deviation σ are listed in Table 2. Statistics are listed both for the entire dataset and for the subset for which $\Delta\epsilon > 0.03$.

The statistics in Table 2 clearly indicate the dependence of retrieval performance on $\Delta\epsilon$. When retrievals for which $\Delta\epsilon \leq 0.03$ are excluded (removing about 29% of all PWV matches), the rms error decreases from 12.9 to 6.4 mm and the linear correlation coefficient increases from 0.68 to 0.89. Moreover, the bias decreases from -3.2 mm to 0.5 mm. Inpection of Fig. 2 indicates that retrievals with low $\Delta\epsilon$ values exhibit large negative biases much more frequently than retrievals for which $\Delta\epsilon > 0.03$. As noted in Section 2.3, the effect of instrumental noise increases as $\Delta\epsilon$ decreases. The statistics in Table 2 thus suggest that instrumental noise is a significant source of retrieval error, one which can be controlled by filtering measures. However, $\Delta\epsilon$-based filters will affect some regions more than others. Over the United States, for example, forested areas exhibit the smallest $\Delta\epsilon$ values [Ruston and Vonder Haar, 2004].

3.2. Oceanic Satellite-based Comparisons

Operational AMSR-E retrievals of PWV over the ocean are retrieved by the algorithm described in *Wentz and Meissner, 2000* and archived by NASA. This product is based on AMSR-E observations at 18.7, 23.8, and 36.5 GHz, as well as estimated values of sea surface temperature and surface-level wind. Operational retrievals are calculated on the same latitude/longitude grid used for the PDP-based method (described in Section 2.3). PWV retrievals produced by this algorithm are compared with PDP-based values for

AMSR-E daytime overpasses on July 3, 2004 for all oceanic regions between 25N, 50N, 130W, and 70W (surrounding North America) in Fig. 3. Larger black diamonds with attached vertical error bars indicate agreement (mean and standard deviation) within PWV bins spaced every five mm. Statistics are also summarized in Table 2.

Overall, the two algorithms yield very similar retrieval results, with typical PWV differences less than about two mm. However, For PWV values of about five cm and greater, binned results indicate biases of approximately three mm and RMS errors of three to five mm. The direction of the bias at high PWV values is consistent with errors produced by neglecting LWP in the development of Eq. 3; i.e., increasing LWP produces a positive bias in retrieved PWV. These errors may diminish in a PDP-based algorithm which retrieves PWV and LWP simultaneously. For PWV values less than five cm, biases between the two products appear negligible and RMS errors are typically less than two mm. Additional studies are planned to identify the source of disagreement at high PWV values (including possible effects of precipitation) and to compare performance in other geographical and seasonal contexts.

4. Conclusions

A new retrieval algorithm for PWV has been developed based on AMSR-E polarization-difference signals at 18.7 and 23.8 GHz. Unlike previous techniques based on microwave observations, the new method is applicable over both ocean and land. The ability of low-frequency microwave radiation to easily penetrate both water and ice clouds allows retrievals of PWV in more general atmospheric conditions than are possible with infrared

observations. This feature is particularly relevant for producing water vapor climatologies which lack a clear-sky bias.

Comparisons with validating datasets demonstrate that the algorithm performs reasonably over both ocean and land. Over land, however, the new technique appears to yield relatively large retrieval errors in scenes where $\Delta\epsilon \leq 0.03$; such regions are associated with dense vegetation. Exclusion of PWV retrievals characterized by low $\Delta\epsilon$ values substantially decreases the retrieval bias and rms error and increases the correlation coefficient. Over oceanic scenes, PWV values agree well with values for the operational AMSR-E product, except at very high PWV values.

Presented results neglect the effect of LWP on the observed polarization-difference signals. PWV retrieval performance should therefore improve if observation-based LWP values are exploited. Ultimately, we plan to merge the PDP-based LWP and PWV retrieval algorithms such that PWV and LWP will be retrieved simultaneously from AMSR-E polarization-difference signals at 18.7, 23.8, 36.5, and 89.0 GHz.

Acknowledgments. SuomiNet data were obtained through the Atmospheric Radiation Measurement (ARM) data archive sponsored by the U.S. Department of Energy, Office of Science, Office of Biological and Environmental Research, Environmental Sciences Division. NCEP Reanalysis data were provided by the NOAA-CIRES Climate Diagnostics Center, Boulder, Colorado, USA, from their Web site at http://www.cdc.noaa.gov/. AMSR-E brightness temperature data were obtained from the National Snow and Ice Data Center through the EOS Data Gateway at http://redhook.gsfc.nasa.gov/ imswww/pub/imswelcome/. AMSR-E Ocean Product data were obtained from Remote Sensing Systems at http://www.remss.com.

References

Albert, P., R. Bennartz, R. Preusker, R. Leinweber, and J. Fischer (2005), Remote sensing of atmospheric water vapor using the Moderate Resolution Imaging Spectroradiometer, *J. Atmos. Ocean. Technol.*, *22*, 309-314.

Braun, J., C. Rocken, and J. Liljegren (2003), Remote sensing of atmospheric water vapor using the Moderate Resolution Imaging Spectroradiometer, *J. Atmos. Ocean. Technol.*, *20*, 606-612.

Deeter, M. N., and J. Vivekanandan (2006), New dual-frequency microwave technique for retrieving liquid water path over land, *J. Geophys. Res.*, *111*, D15209, doi:10.1029/2005JD006784.

Engelen, R. J., and G. L. Stephens (1999), Characterization of water-vapour retrievals from TOVS/HIRS and SSM/T-2 measurements, *Q. J. R. Meteorol. Soc.*, *125*, 331-351.

Gao, B.-C., and Y. J. Kaufman (2003), Water vapor retrievals using Moderate Resolution Imaging Spectroradiometer near-infrared channels, *J. Geophys. Res.*, *108*, 4389, doi:10.1029/2002JD003023.

Kawanishi, T., et al. (2003), The Advanced Microwave Scanning Radiometer for the Earth Observing System (AMSR-E), NASDA's contribution to the EOS for global energy and water cycle studies, *IEEE Trans. Geosci. Remote Sens.*, *41*, 184-194.

Lin, B. and P. Minnis (2000), Temporal variations of land surface microwave emissivities over the Atmospheric Radiation Measurement program Southern Great Plains site, *J. Appl. Met.*, *39*, 1103-1116.

Prigent, C., W. B. Rossow, and E. Matthews (1997), Microwave land surface emissivities estimated from SSM/I observations, *J. Geophys. Res.*, *102*, 21,867-21,890.

Ruston, B. C., and T. H. Vonder Haar (2004), Characterization of summertime microwave emissivities from the Special Sensor Microwave Imager over the conterminous United States, *J. Geophys. Res.*, *109*, D19103, doi:10.1029/2004JD004890.

Seemann, S., J. Li, W. P. Menzel, and L. Gumley (2003), Operational retrieval of atmospheric temperature, moisture, and ozone from MODIS infrared radiances, *J. Appl. Met.*, *42*, 1072-1091.

Simpson, J. J., et al. (2001), The NVAP global water vapor data set: independent cross-comparison and multi-year variability, *Remote Sens. Environ., 76*, 112-129.

Sohn, B.-J., and E. A. Smith, (2003), Explaining sources of discrepancy in SSM/I waer vapor algorithms, *J. Climate, 16*, 3229-3255.

Stephens, G. L., (1990), On the relationship between water vapor over the oceans and sea surface temperature, *J. Climate, 3*, 634-645.

Stephens, G. L., D. L. Jackson, and J. J. Bates (1994), A comparison of SSM/I and TOVS column water vapor data over the global oceans, *Meteorol. Atmos. Phys., 54*, 183-201.

Trenberth, K. E., J. Fasullo, and L. Smith (2005), Trends and variability in column-integrated atmospheric water vapor, *Clim. Dyn., 24*, 741-758.

Ware, R. H., et al., (2000), SuomiNet: A real-time national GPS network for atmospheric research and education, *Bull. Amer. Meteor. Soc., 81*, 677-694.

Wentz, F. J., and T. Meissner (2000), AMSR Ocean Algorithm: Algorithm Theoretical Basis Document, Ver. 2, Remote Sensing Systems Technical Proposal RSS121599A-1

(available at http://eospso.gsfc.nasa.gov/eos_homepage/for_scientists/atbd).

Wilheit, T., C. D. Kummerow, and R. Ferraro (2003), Rainfall algorithms for AMSR-E, *IEEE Trans. Geosci. Rem. Sens., 41,* 204-214.

Table 1. Regression coefficients (as determined by applying multiple linear regression to Eq. 1) and parameterization error σ as described in Section 2.1. Values of β and σ assume that ΔT_B values are expressed in K.

Channel	β_0	$\beta_1(K^{-1})$	β_2 (mm^{-1})	β_3 (mm^{-1})	σ
18.7 GHz	4.39	0.00423	-0.275	-0.00585	0.0110
23.8 GHz	4.39	0.00414	-0.450	-0.0179	0.0143

Table 2. Validation statistics (number of paired PWV values N, least-squares best-fit slope m and offset b, linear correlation coefficient r, and overall bias and standard deviation σ) corresponding to data described in sections 3.1 and 3.2 and presented in Figs. 3 and 4. Entries for "Filtered GPS" indicate statistics of GPS matchups for which retrieved value of $\Delta\epsilon > 0.03$ (see Section 3.1).

Validation Data	N	m	b (mm)	r	bias (mm)	σ (mm)
All GPS	25,637	1.009	-3.34	0.682	-3.18	12.85
Filtered GPS	18,110	1.058	-0.59	0.887	0.45	6.35
AMSR-E "OPS"	5,884	1.088	-2.05	0.987	0.78	2.22

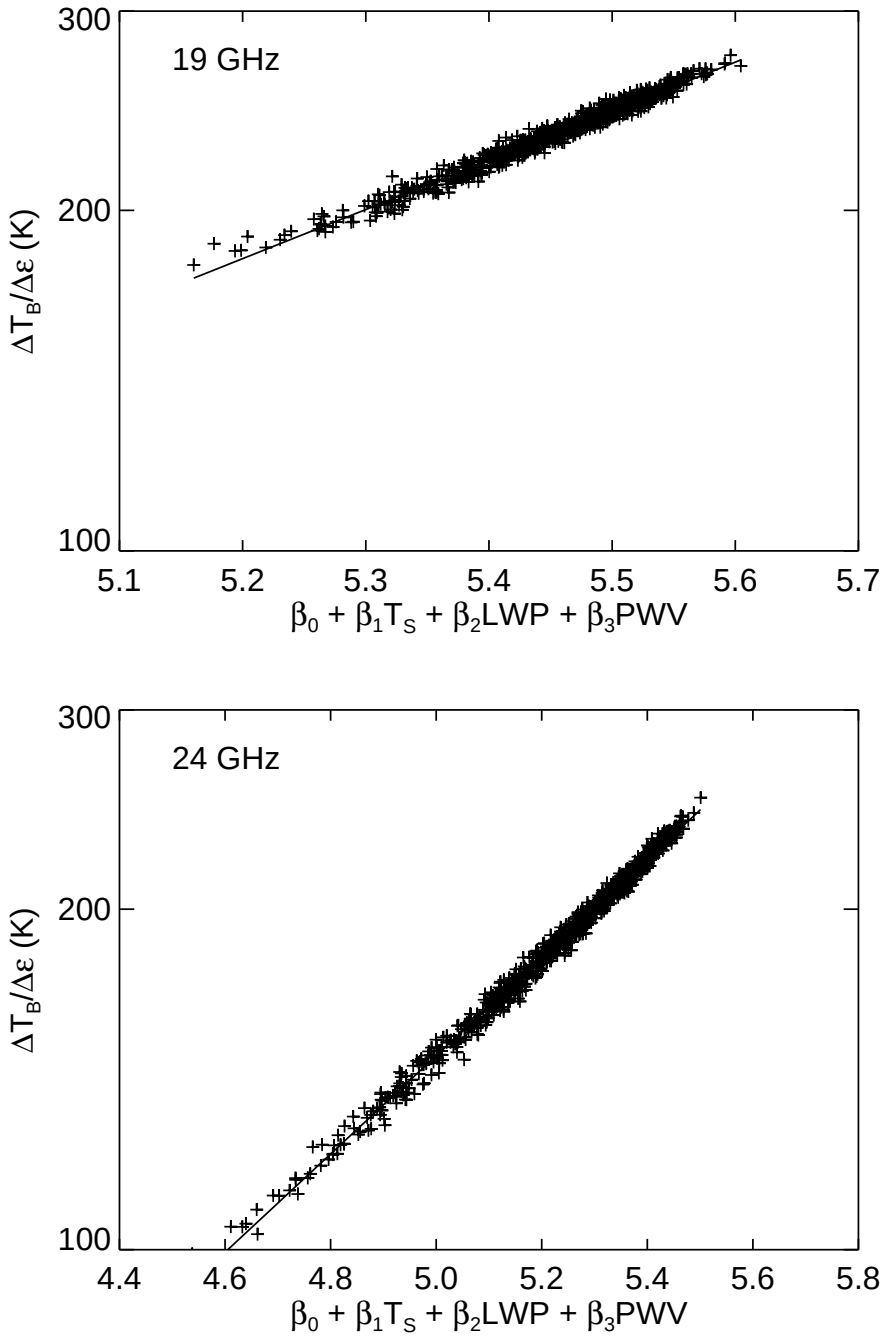

Figure 1. Results of multiple linear regression applied to Eq. 1 for both the 18.7 and 23.8 GHz AMSR-E polarization-difference signals. Plotted points indicate results of radiative transfer simulations described in Section 2.1. Solid line indicates best fit as determined by regression analysis.

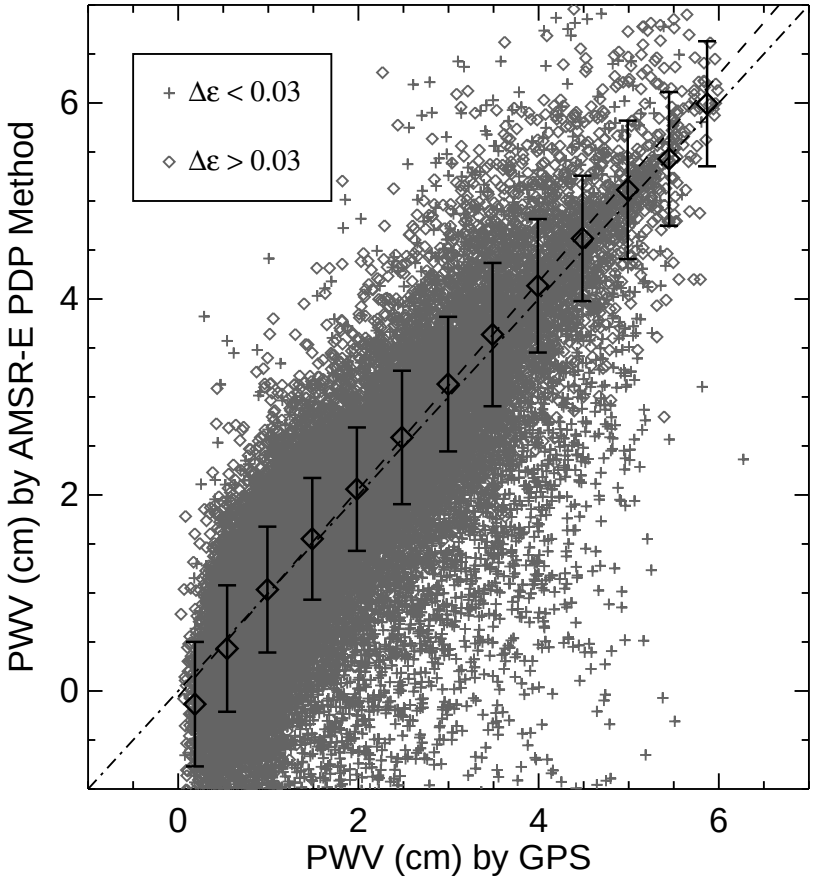

Figure 2. Comparison of AMSR-E PDP-based PWV retrievals with GPS-based PWV retrievals over North American land surfaces for all of 2004. Larger black diamonds and attached error bars indicate statistics of binned retrievals (using bins 0.5 cm wide) where $\Delta\epsilon > 0.03$.

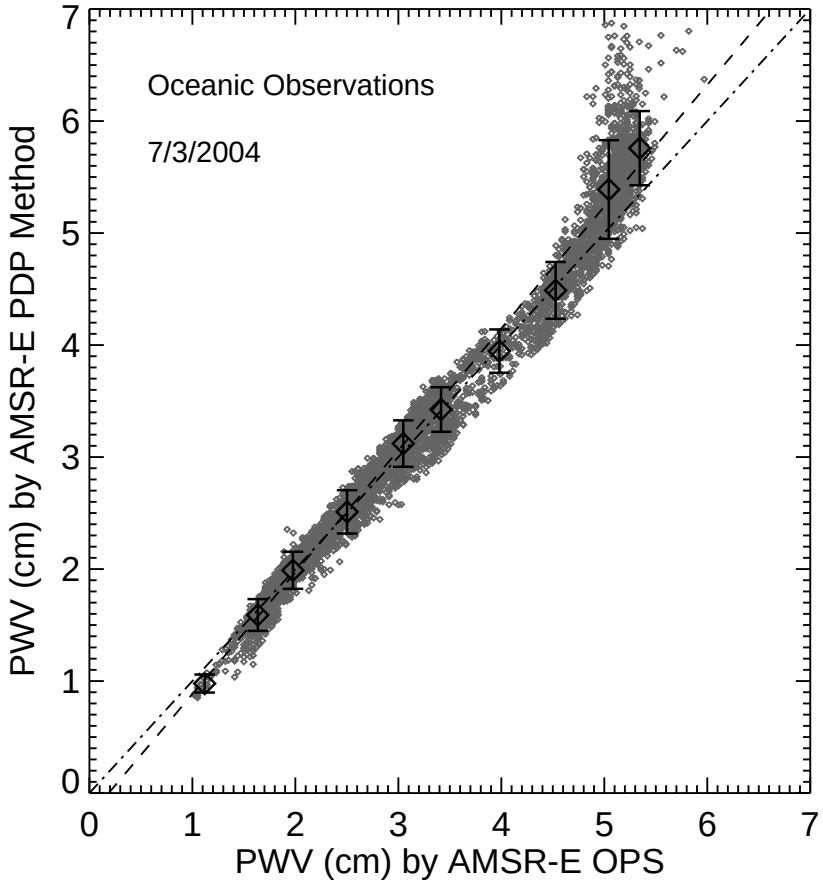

Figure 3. Comparison of AMSR-E PDP-based PWV retrievals with operational AMSR-E Ocean Product PWV values over oceanic regions adjacent to North America for July 3, 2004.